Monthly Notices
of the
ROYAL ASTRONOMICAL SOCIETY

Mon. Not. R. Astron. Soc. **403,** 1331–1338 (2010) doi:10.1111/j.1365-2966.2009.16088.x

The low wind expansion velocity of metal-poor carbon stars in the Halo and the Sagittarius stream★†

Eric Lagadec,[1]‡ Albert A. Zijlstra,[1] Nicolas Mauron,[2] Gary Fuller,[1] Eric Josselin,[2] G. C. Sloan[3] and A. J. E. Riggs[4,5]

[1]*Jodrell Bank Center for Astrophysics, Alan Turing Building, School of Physics and Astronomy, The University of Manchester, Oxford Street, Manchester M13 9PL*
[2]*Goupe d'Astrophysique, UMR 5024 CNRS, Case CC72, Place Bataillon, 34095 Montpellier Cedex 5, France*
[3]*Department of Astronomy, Cornell University, 108 Space Sciences Building, Ithaca NY 14853-6801, USA*
[4]*Astronomy Department, Yale University, 260 Whitney Avenue, New Haven, CT 06511, USA*
[5]*NSF REU Research Assistant, Department of Astronomy, Cornell University, NY 14853-6801, USA*

Accepted 2009 November 20. Received 2009 November 12; in original form 2009 August 17

ABSTRACT

We report the detection, from observations using the James Clerk Maxwell Telescope, of CO $J = 3 \rightarrow 2$ transition lines in six carbon stars, selected as members of the Galactic Halo and having similar infrared colours. Just one Halo star had been detected in CO before this study. Infrared observations show that these stars are red ($J - K > 3$), due to the presence of large dusty circumstellar envelopes. Radiative transfer models indicate that these stars are losing mass with rather large dust mass-loss rates in the range 1–3.3 $\times$ 10^{-8} $M_{\odot}$ yr^{-1}, similar to what can be observed in the Galactic disc. We show that two of these stars are effectively in the Halo, one is likely linked to the stream of the Sagittarius Dwarf Spheroidal galaxy (Sgr dSph), and the other three stars certainly belong to the thick disc. The wind expansion velocities of the observed stars are lower compared to carbon stars in the thin disc and are lower for the stars in the Halo and the Sgr dSph stream than in the thick disc. We discuss the possibility that the low expansion velocities result from the low metallicity of the Halo carbon stars. This implies that metal-poor carbon stars lose mass at a rate similar to metal-rich carbon stars, but with lower expansion velocities, as predicted by recent theoretical models. This result implies that the current estimates of mass-loss rates from carbon stars in Local Group galaxies will have to be reconsidered.

Key words: stars: carbon – circumstellar matter – infrared: stars – stars: mass loss.

1 INTRODUCTION

Stars with initial masses in the range of 0.8–8 $M_{\odot}$ end their life with a phase of catastrophic mass-loss. During the asymptotic giant branch (AGB) phase, they develop a superwind leading to mass-loss rates up to 10^{-4} $M_{\odot}$ yr^{-1}. This superwind enriches the interstellar medium (ISM) with newly synthesized elements.

The mass-loss mechanism of AGB stars is likely due to pulsations from the star and radiation pressure on dust grains. Shocks due to pulsation extend the atmosphere, so that the material ejected by the star becomes dense and cold enough for dust to form. Due to its opacity, dust absorbs the radiation from the star and is driven away by radiation pressure, carrying the gas along through friction. Theoretical models (Winters et al. 2000) show that the mass-loss evolves from a pulsation driven regime characterized by a low mass-loss rate and a slow expansion velocity to a dust-driven regime with a high mass-loss rate and a high expansion velocity (>5 km s^{-1}).

Studying the effect of metallicity on the mass-loss process is important to understand the formation of dust around AGB stars in the early Universe. At low metallicity, less seeds are present for dust formation, so one might expect dust formation to be less efficient and thus the mass-loss rates to be lower.

A theoretical study by Bowen & Willson (1991) predicts that for metallicities below [Fe/H] $= -1$ dust-driven winds fail, and the wind must stay pulsation driven. However, observational evidence for any metallicity dependence is still very limited (Zijlstra 2004). More recent observational (Groenewegen et al. 2007) and theoretical studies (Mattsson et al. 2008; Wachter et al. 2008) indicate that

★Based on observations made at the James Clerk Maxwell Telescope under program M08AU01.
†Based on observations made at the Very Large Telescope at Paranal Observatory under the program 082.D-0836.
‡E-mail: eric.lagadec@manchester.ac.uk

the mass-loss rates from carbon stars in metal-poor environments are similar to our Galaxy.

To obtain the first observational evidence on mass-loss rates at low metallicity, we have carried out several surveys with the *Spitzer Space Telescope* of stars in nearby dwarf galaxies. These show significant mass-loss rates down to $Z = 1/25\,Z_{\odot}$ (Lagadec et al. 2007; Matsuura et al. 2007; Sloan et al. 2009), but only for carbon-rich stars. The current evidence indicates that oxygen-rich stars have lower mass-loss rates at lower metallicities. For carbon stars, no evidence for a dependency of mass-loss rate on metallicity has yet been uncovered. Consequently, (Lagadec & Zijlstra 2008) have proposed that the carbon-rich dust plays an important role in triggering the AGB superwind.

The main uncertainty arises from the unknown expansion velocity. This parameter is needed to convert the density distribution to a mass-loss rate. The expansion velocity is also in itself a powerful tool. Hydrodynamical simulations (Winters et al. 2000) have shown that radiation-driven winds have expansion velocity in excess of $5\,\mathrm{km\,s^{-1}}$, while pulsation-driven winds are slower.

There is some evidence that expansion velocities are lower at low metallicity, from measurement of OH masers (Marshall et al. 2004). However, OH masers are found only in oxygen-rich stars, which appear to have suppressed mass-loss at low metallicities. We lack equivalent measurements for metal-poor carbon-rich stars, which do reach substantial mass-loss rates. For these, the only available velocity tracer is CO. Currently, extra-galactic stars are too distant for CO measurements. However, there are a number of carbon stars in the Galactic Halo, which are believed to have similarly low metallicity. One CO measurement exists for a Galactic Halo star: its expansion velocity has been estimated to be $\sim 3.2\,\mathrm{km\,s^{-1}}$ through the ^{12}CO $J = 2 \rightarrow 1$ transition (Groenewegen, Oudmaijer & Ludwig 1997). This is much lower than typical expansion velocities, which are in the range 10–40 $\mathrm{km\,s^{-1}}$ for stars with similar colours, and thus optical depths (Fig. 1).

A large number of metal-poor carbon stars have recently been discovered in the Galactic Halo (Totten & Irwin 1998; Mauron et al. 2004, 2005; Mauron, Kendall & Gigoyan 2007). These stars may have been stripped from the Sagittarius Dwarf Spheroidal galaxy (Sgr dSph), which has a metallicity of [Fe/H] ~ -1.1 (Van de Bergh 2000). These stars are the closest metal-poor carbon stars known, and they are bright enough to be detected in CO using ground-based millimetre telescopes.

We have carried out observations of six Halo carbon stars in the CO $J = 3 \rightarrow 2$ transition. Here, we report the results of these observations.

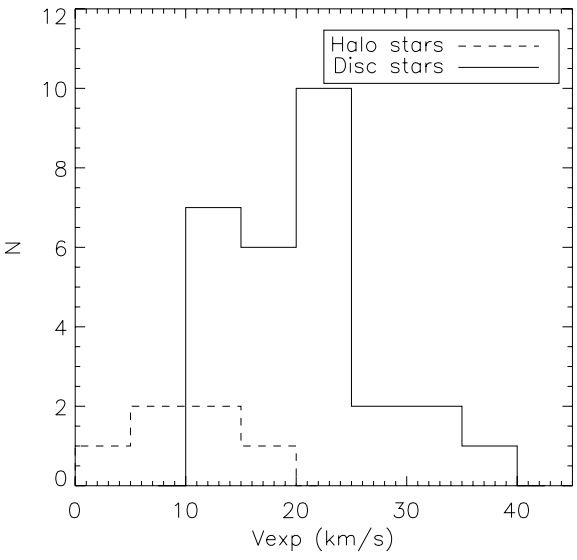

Figure 1. Distribution of the expansion velocity for the observed Halo carbon stars compared with stars from the disc with similar $J - K$ colours.

2 SAMPLE SELECTION

Mauron et al. (2004, 2005, 2007) and Mauron (2008) have discovered ~ 100 carbon stars in the Galactic Halo, adding to the sample of $\sim$50 described by Totten & Irwin (1998). All of these stars are spectroscopically confirmed carbon stars. Only the brightest can be detected in the sub-millimetre range. We selected the six stars with the highest *Infrared Astronomical Satellite* (*IRAS*) 12 μm flux observable with the James Clerk Maxwell Telescope (JCMT, Mauna Kea, Hawaii). The emission from an AGB star at 12 μm is due to thermal emission from the dust in the envelope. Thus, one expects the stars with the largest 12 μm flux to be the brightest in CO. All the observed stars have $3 < J - K < 4$ and have thus a similar dust optical depth and a large circumstellar dusty envelope.

Table 1 describes the observational properties of the selected stars. One of these stars, IRAS 12560+1656 (Beichman et al. 1990), is the only Halo carbon star that had previously been detected in CO $J = 2 \rightarrow 1$ (by Groenewegen et al. 1997).

3 OBSERVATIONS AND DATA REDUCTION

We observed the CO $J = 3 \rightarrow 2$ (345 GHz) line emission from the six selected carbon stars from the JCMT using the heterodyne focal-plane array receiver (HARP; Smith et al. 2008). Observations were carried with a bandwidth of 1 GHz and a frequency resolution of 0.977 MHz, giving a velocity coverage of $\pm 400\,\mathrm{km\,s^{-1}}$. To increase the signal-to-noise ratio of our observations, we used a 30 arcsec beam switch to keep one detector on the source at all times. We used the Starlink software to reduce the resulting data. Fig. 2 shows the six CO 3–2 lines we detected.

We obtained mid-infrared photometric observations of two stars from our sample using the Very Large Telescope (VLT) Imager and Spectrometer for mid-Infrared (VISIR; Lagage et al. 2004) on the Very Large Telescope (VLT). The observations were taken using four filters centred at 8.59 μm (PAH1, $\Delta\lambda = 0.42$ μm), 11.25 μm (PAH2, $\Delta\lambda = 0.59$ μm), 13.04 μm (Ne II$_2$, $\Delta\lambda = 0.22$ μm) and 17.65 μm (Q1, $\Delta\lambda = 0.83$ μm). We used the standard mid-infrared chop-and-nod technique to remove the background emission from the telescope and sky. Standard stars were observed just after each observation for flux calibration. The data were reduced using the Interactive Data Language (IDL) routines developed and described by Lagadec et al. (2008).

4 CO LINE PROPERTIES

Fig. 2 shows that the six lines we detected have parabolic profiles, which arise when the envelopes of the observed stars are spherical, unresolved by the telescope, have a constant expansion velocity V_{exp}, and the CO 3–2 line is optically thick (Knapp & Morris 1985). This can be described as

$$T_A^*(V) = T_A^*(\mathrm{peak}) \left[1 - \left(\frac{\mathrm{V} - \mathrm{V_c}}{\mathrm{V_0}} \right)^2 \right], \quad (1)$$

Table 1. Observed Halo stars targets: names, adopted coordinates, photometry and distance. J, H, K_s are taken from 2MASS. $f_{8.59}$, $f_{13.04}$ and $f_{17.65}$ are the VISIR/VLT flux at 8.59, 13.04 and 17.65 μm respectively. f_{12} is the *IRAS* 12 μm flux. Z is the distance above the Galactic plane.

IRAS name	Other name	RA	Dec. (J2000)	K (mag)	$J-K$ (mag)	$f_{8.59}$ (Jy)	$f_{13.04}$ (Jy)	$f_{17.65}$ (Jy)	f_{12} (Jy)	[12] (mag)	Z (kpc)
IRAS 04188+0122	CGS 6075	04 21 27.25	+01 29 13.4	6.420	3.280	4.99	2.67	1.64	3.37	2.31	−2.63
IRAS 08427+0338	CGS 6306	08 45 22.27	+03 27 11.2	6.255	3.410	–	–	–	6.50	1.60	2.03
IRAS 11308−1020	CGS 3052	11 33 24.57	−10 36 58.6	4.568	3.830	–	–	–	57.37	−0.77	1.41
IRAS 16339−0317	CGS 3716	16 36 31.70	−03 23 37.5	6.098	3.906	12.49	10.83	5.60	14.57	0.72	1.73
IRAS 12560+1656	CGS 6500	12 58 33.50	+16 40 12.0	7.820	3.480	–	–	–	0.77	3.91	8.96
IRAS 18120+4530		18 13 29.6	+45 31 17.0	6.710	3.809	–	–	–	7.86	1.39	2.20

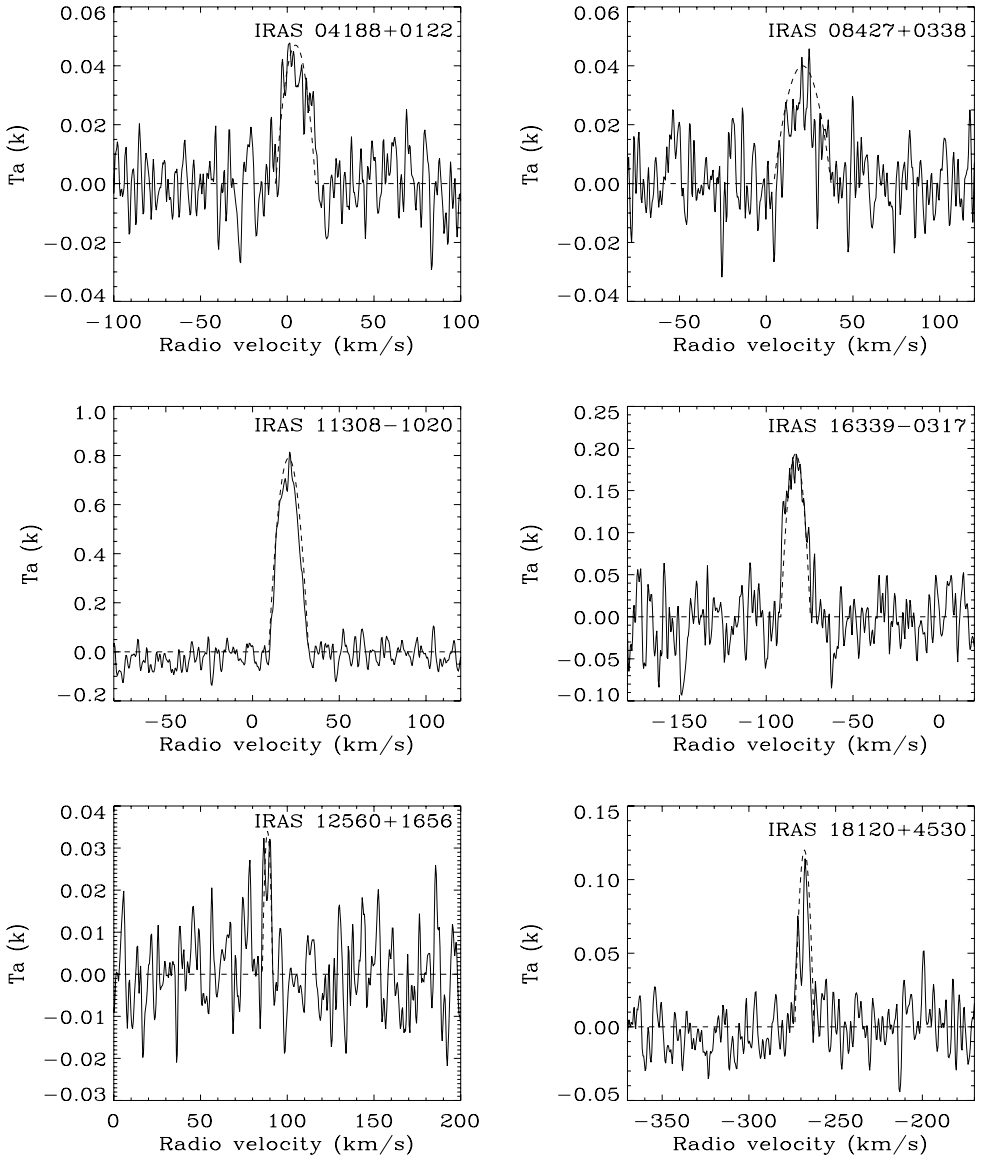

Figure 2. JCMT CO 3–2 line of the six observed stars. The dashed line represent the best model fit to the data. The velocities in abscissa are V_{LSR}.

where T_A^*(peak) is the peak emission temperature, V_0 is the expansion velocity of the envelope, and V_C the velocity of the line. We fitted this function to the observed data with a least-squares technique. Table 2 lists the resulting properties of the observed lines. The CO lines detected for IRAS 12560+1656 is rather weak, but can be considered as a real detection as it was already detected in another transition by Groenewegen et al. (1997).

Fig. 1 shows the distribution of expansion velocities for our sample. As expected, the flux measured in the CO 3–2 line correlates strongly with the *IRAS* 12 μm flux (Fig. 3). The best linear fit to the data is obtained for

$$F_{CO} = 0.194 \pm 0.009 \times f_{12} - 0.314 \pm 0.214. \quad (2)$$

Table 2. CO J = 3–2 line properties of the observed Halo stars. Typical errors on the expansion velocity estimates are 0.1 km s^{-1} for the stars with expansion velocities above 10 km s^{-1} and 0.2 s^{-1} for the other ones.

Adopted name	Peak (K)	$V_{\rm LSR}$ (km s^{-1})	$V_{\rm exp}$ (km s^{-1})	FWHM (km s^{-1})	Flux (K km s^{-1})	rms (K)	Integration time (min)
IRAS 04188+0122	0.04	4.8	11.5	17.3	0.77	0.009	616
IRAS 08427+0338	0.03	20.9	16.5	17.4	0.55	0.010	45
IRAS 11308−1020	0.79	20.8	11.5	12.9	10.86	0.049	90
IRAS 16339−0317	0.19	−83.1	8.5	12.6	2.59	0.030	182
IRAS 12560+1656	0.03	88.6	3.	4.5	0.14	0.008	453
IRAS 18120+4530	0.08	−268.0	6.5	8.3	0.72	0.019	227

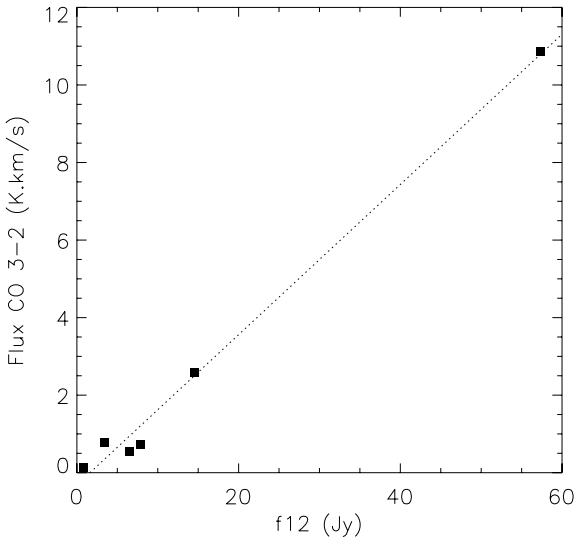

Figure 3. The linear correlation between the *IRAS* 12 μm flux and the observed CO $J = 3$–2 flux.

5 DUST MASS-LOSS RATES

Two techniques are usually used to estimate dust mass-loss rates from AGB stars: by measuring the near- and mid-infrared flux of the stars (Whitelock et al. 1994, 2006; Lagadec et al. 2008) or by using radiative transfer models. We apply both methods here. We estimated the mass-loss rates by measuring the $K_{\rm s} - [12]$ colour, where K_s is the Two Micron All Sky Survey (2MASS) 2.16 μm magnitude and [12] the *IRAS* 12 μm magnitude, according to the relation from Whitelock et al. (2006):

$$\begin{aligned}\log(\dot{M}_{\rm total}) = &-7.668 + 0.7305(K - [12]) \\ &- 5.398 \times 10^{-2}(K - [12])^2 \\ &+ 1.343 \times 10^{-3}(K - [12])^3, \end{aligned} \quad (3)$$

where [12] is the *IRAS* 12 μm magnitude assuming a zero-magnitude flux of 28.3 Jy.

We obtained an alternative estimate of the dust mass-loss rates using a radiative transfer model. We used the radiative transfer code DUSTY (Ivezić & Elitzur 1997). This code solves the one-dimensional problem of radiation transport in a dusty environment. For all of our models, we assume that the irradiation comes from a point source (the central star) at the centre of a spherical dusty envelope. The circumstellar envelope is filled with material from a radiatively driven wind. All of the stars are carbon-rich, and the dust consists of amorphous carbon. We did not add SiC to our model, except for IRAS 04188+0122 and IRAS 16339−0317, for which a fit was impossible without SiC. Optical properties for these dust grains are taken from Hanner (1988) and Pégourié (1988) for amorphous carbon and SiC, respectively. The grain size distribution is taken as a typical Mathis–Rumpl–Nordsieck (MRN) distribution, with a grain size a varying from 0.0005 to 0.25 μm distributed according to a power law with $n(a) \propto a^{-q}$ with $q = 3.5$ (Mathis et al. 1977). The outer radius of the dust shell was set to 10^3 times the inner radius; this parameter has a negligible effect on our models.

To model the emission from the central star, we used a hydrostatic model including molecular opacities (Loidl, Lançon & Jørgensen 2001; Groenewegen et al. 2007). Our aim was to fit the spectral energy distribution, defined by the 2MASS photometry (J, H and K), our VISIR mid-infrared data, and the *IRAS* photometry (at 12 and 25 μm) to estimate the dust mass-loss rates. We fixed the dust temperature at inner radius (1220 K), the mass ratio of SiC to amorphous (0 per cent) carbon dust and the effective temperature of the central star, $T_{\rm eff}$ (2800 K), unless a satisfactory fit could not be obtained with these parameters.

DUSTY gives total (gas+dust) mass-loss rates assuming a gas-to-dust ratio of 200. Estimating the gas-to-dust ratio of these stars is beyond the scope of this paper and will be the subject of a forthcoming paper using CO observations of these stars in other transitions and *Spitzer* spectra. We thus prefer to estimate dust mass-loss rates. The dust mass-loss rate can be obtained by dividing by the gas-to-dust mass ratio, assuming that the gas and dust expansion velocities are the same. Here, we prefer to talk about dust mass-loss rates as inputs from our models as we are fitting infrared colours, and thus dust emission. The expansion velocity is an output for the DUSTY models, and we scaled our results using the expansion velocities we measured. Table 3 and Fig. 4 give the results of the fits. The *IRAS* 12 μm flux is an outlier for IRAS 16339−0317. This is certainly due to variability or to the fact that the aperture of the *IRAS* satellite is larger than the VISIR one.

6 DISCUSSION

6.1 Mass-loss and evolution

The detection of resolved CO lines in our six targets indicate that all of these stars are losing mass. Our VISIR observations, as well as *IRAS* and 2MASS observations, show that these stars are very red, which indicates the presence of circumstellar dust. To study the impact of the mass-loss on the evolution of the studied stars, we compared the measured mass-loss rates with nuclear reaction rates and the classical single-scattering limit (see e.g. van Loon, Zijlstra & Groenewegen 1999; Lagadec et al. 2008).

Fig. 5 shows the total (gas+dust) mass-loss rate as a function of the absolute magnitude. The absolute magnitude is taken from our DUSTY models. The total mass-loss rate is also an output from our DUSTY models, assuming a typical gas-to-dust mass ratio of 200. The

Table 3. Dust mass-loss rates for the observed stars and parameters obtained from our DUSTY models. $\dot{M}_{\rm col}$ and $\dot{M}_{\rm DUSTY}$ are the dust mass-loss rates (in $M_\odot$ yr^{-1}) from Lagadec et al. (2008) and our DUSTY models, respectively. The distance we adopted is the average between the distances D_1 and D_2 described in Section 6.2

Target	Luminosity ($L_\odot$)	$\dot{M}_{\rm DUSTY}$ (10^{-8} $M_\odot$ yr^{-1})	$T_{\rm eff}$ (K)	$T_{\rm in}$ (K)	SiC/AMC	τ (0.55 μm)	$\dot{M}_{\rm col}$ (10^{-8} $M_\odot$ yr^{-1})	Distance (kpc)
IRAS 04188+0122	8221	1.0	2800	1200	0.1	10.	1.6	6.2
IRAS 08427+0338	10124	1.8	2800	1200	0.	10.	2.5	5.6
IRAS 11308−1020	16793	2.9	2800	1200	0.	10.	3.9	2.4
IRAS 16339−0317	6976	1.8	2800	1200	0.	17.8	4.0	4.8
IRAS 12560+1656	7563	0.4	2800	1200	0.	10.	1.4	11.4
IRAS 18120+4530	13391	1.4	2800	1200	0.1	10.	3.9	6.5

dotted line shows the rate at which mass is consumed by nuclear burning and the dashed line the classical single-scattering limit as described by Lagadec et al. (2008). This shows that no multiple scattering is needed to explain the observed dust mass-loss rates. The mass-loss rates we measure are also well above the nuclear burning rate line, indicating that the evolution of these stars will be governed by the mass-loss process. Similar conclusions were drawn from observations of metal-poor AGB stars in the Large Magellanic

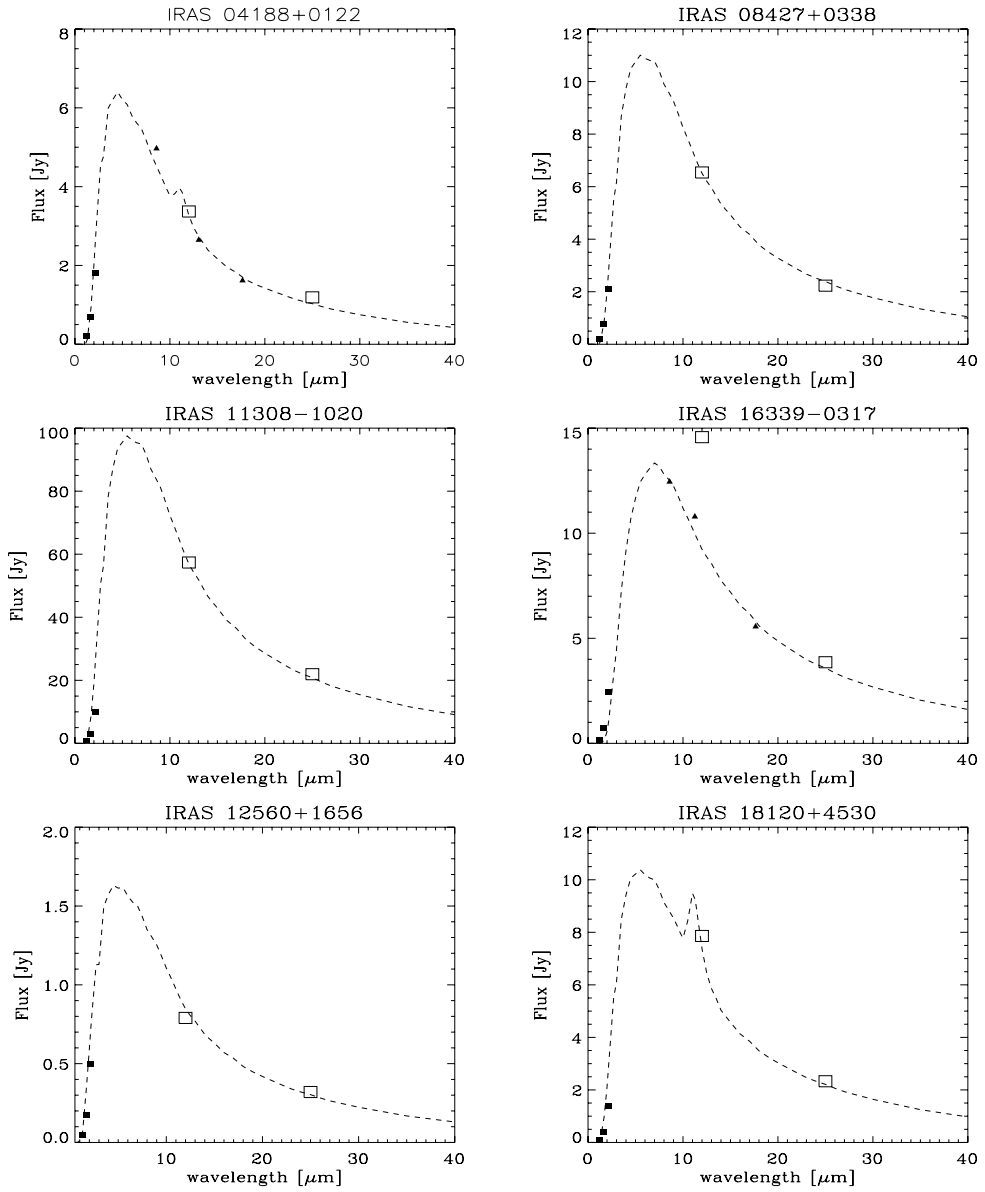

Figure 4. Radiative transfer DUSTY models of the spectral energy distributions of the observed stars. The dashed lines represent our best models, and the symbols are flux from 2MASS, *IRAS* (12 and 25 μm) and our VISIR observations. Filled squares, open squares and triangles represent 2MASS, *IRAS* and VISIR/VLT data, respectively.

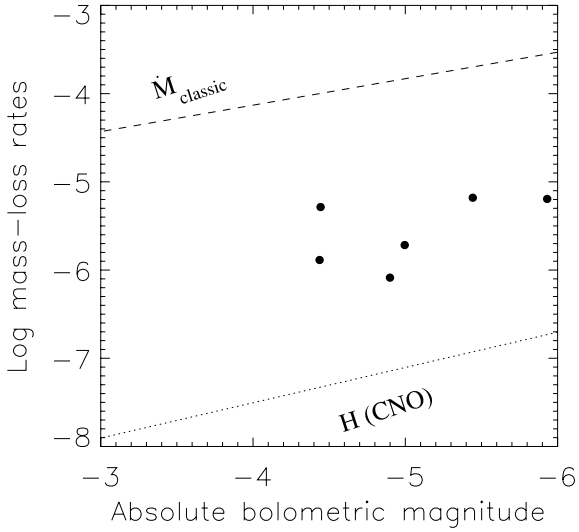

Figure 5. Total (gas+dust) mass-loss rate as a function of the absolute bolometric magnitude.

Cloud (LMC), Fornax and Sgr dSph (van Loon et al. 1999; Lagadec et al. 2008).

6.2 Distances

Most of the methods to determine mass-loss rates rely on an accurate distance to the observed stars. To determine these distances, we applied three methods. Two are based on near-infrared colours; the third is the period–luminosity relationship.

The first method uses the infrared colours of the observed stars, using the relation between M_K and $J - K$ determined by Sloan et al. (2008). They found from a sample of carbon stars in the Small Magellanic Cloud (SMC) that

$$M_K = -9.18 + 0.395(J - K). \quad (4)$$

Mauron (2008) compared the near-infrared 2MASS photometry of stars in the Halo and the LMC and found a different relationship from the one above between $J - K$ and M_K. Their relation gives fainter M_K values at a given $J - K$ colour than that of Sloan et al., with the difference increasing with redder colours. We have recalibrated the relation for the LMC, using the samples of stars confirmed to be carbon-rich with the Infrared Spectrograph on *Spitzer* by Zijlstra et al. (2006), Buchanan et al. (2006), Leisenring, Kemper & Sloan (2008) and Sloan et al. (2008). We find that

$$M_K = -9.94 + 0.754(J - K), \quad (5)$$

for $J - K$ colours greater than 2.0. This calibration of the $J - K$ relation is our second method. Fig. 6 compares the SMC and LMC calibrations of the relation between M_K and $J - K$.

The scatter in the LMC sample is 0.81 mag about the fitted line, compared to 0.51 mag for the SMC sample. The two fitted lines yield nearly identical distances at $J - K = 2$, but as the colour grows redder, the samples diverge from each other. At $J - K = 5$, the difference in M_K is a full magnitude. For the colours in our sample, the two methods yield results differencing by 0.41–0.64 mag, comparable to the spread in the SMC sample. The different slopes in the two samples may result from their different metallicities, but that is only speculation on our part.

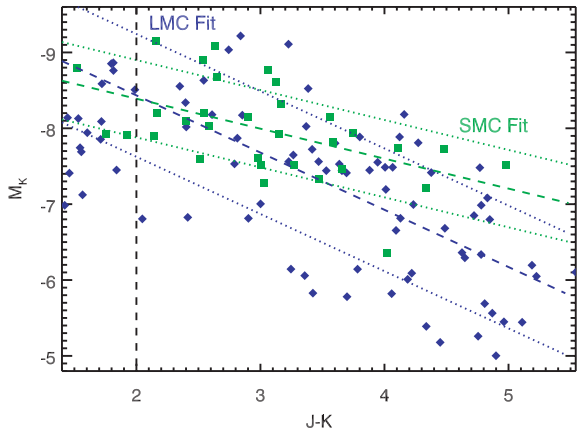

Figure 6. Absolute K magnitude (M_K) of carbon stars as a function of their $J - K$ infrared colours. Diamonds and squares represent LMC and SMC carbon stars respectively. The vertical dashed line represent the limit under which relation equation (5) is no longer valid.

The third method utilizes the period–luminosity relation for carbon Miras described by Feast, Whitelock & Menzies (2006),

$$M_{bol} = -2.54 \log P + 2.06. \quad (6)$$

With an uncertainty of 0.24 mag. We derived the bolometric magnitudes using the equation for bolometric correction derived by Whitelock et al. (2006), after converting all of the photometry to the South African Astronomical Observatory (SAAO) system as described by Lagadec et al. (2008),

$$BC_K = +0.972 + 2.9292 \times (J - K) - 1.1144 \times (J - K)^2 + 0.1595 \times (J - K)^3 - 9.5689\,10^3 (J - K)^4. \quad (7)$$

Table 4 presents the obtained distances, D_1, D_2 and D_3, respectively. For those stars without periods, the final estimated distance is the average of D_1 and D_2. For those stars with periods, the D_1 and D_2 values bracket D_3 in two of the three cases. Consequently, we first averaged D_1 and D_2, then averaged the result with D_3 to arrive at our final estimate of the distance. The uncertainties in the final estimated distances are the standard deviation of the individual distances.

6.3 Galactic location of the stars

Knowing the distance to the stars and their V_{lsr} allows us to study their location in the Galaxy. All six stars examined here have been classified previously as members of the Halo, based on their distances from the Galactic plane. Our CO observations give us velocity information for these stars, which we can compare to Galactic rotation models. Table 4 lists the Galactic coordinates l and b.

Fig. 7 shows the location of our six carbon stars on an Aitoff projection. The dashed line schematically represents the Sgr dSph orbit (Ibata et al. 2001). One of our stars, IRAS 12560+1656, lies very close to this orbit. Its V_{lsr} is in the range of the observed V_{lsr} for stars in the Sgr dSph stream. IRAS 12560+1656 very likely belongs to this stream. Our observations are thus certainly the first CO observations of an extragalactic AGB star. Two other stars, IRAS 16339−0317 and IRAS 18120+4530, have large negative V_{lsr}, fully consistent with membership in the Halo. Finally, IRAS 04188+0122, IRAS 08427+0338 and IRAS 11308−1020 have a distance, location and V_{lsr} consistent with membership in the thick disc. These three last stars thus have a metallicity between that of the thin Galactic disc and the Galactic Halo, the average metallicity

Table 4. Galactic location of our observed stars. D_1, D_2 and D_3 are the distance to the sun using methods described by Sloan et al. (2008), Mauron et al. (2008) and the period-luminosity relation respectively. This last method was not applied for three stars without known periods from the Northern Sky Variability Survey (NSVS; Woźniak et al. 2004).

Adopted name	l	b	Period (d)	D_1 (kpc)	D_2 (kpc)	D_3 (kpc)	$\langle D \rangle$ (kpc)
IRAS 04188+0122	192.1775	−31.9867	359	7.3	6.0	6.4	6.5±0.6
IRAS 08427+0338	223.4859	+26.8173	288	6.6	5.3	5.1	5.5±0.8
IRAS 11308-1020	273.6969	+47.7772	–	2.8	2.1	–	2.5±0.5
IRAS 16339-0317	012.7346	+27.7944	–	5.6	4.2	–	4.9±1.0
IRAS 12560+1656	312.2528	+79.4127	–	13.3	10.7	–	12.0±1.9
IRAS 18120+4530	073.0530	+25.3482	408	7.6	5.7	6.7	6.7±0.9

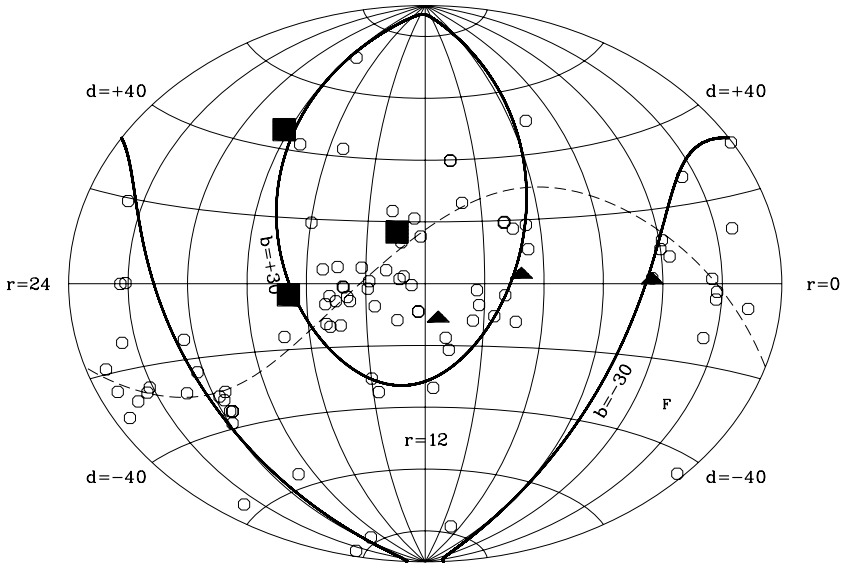

Figure 7. The location of the six carbon stars on an Aitoff projection of the sky. Open circles represent Halo carbon stars from Mauron et al. (2004, 2005, 2007) and Totten & Irwin (1998) with $J - K > 1.2$ and $K > 6$ to eliminate carbon stars in the disc. Filled symbols represent the six stars in our sample.

of the thin disc being ∼−0.17 while the one of the thick disc is ∼−0.48 (Soubiran, Bienaymé & Siebert 2003). Our sample thus contains three metal-poor AGB stars and three AGB stars with intermediate metallicity.

6.4 Low expansion velocities in the Halo

The present observations allow us to directly measure the expansion velocity for a sample of carbon stars in the Halo. The stars we observed are quite red ($3 < J - K < 4$), and have substantial circumstellar dusty envelopes responsible for the observed reddening. Our measured expansion velocities are in the range 3–16.5 km s^{-1}. The expansion velocity of carbon stars increases during the evolution on the AGB (Schöier 2007), i.e. when the dusty envelope becomes optically thicker. To compare the expansion velocities, we measured in Halo carbon stars with carbon stars in the disc, we took a sample of carbon stars in the disc with colours similar to our sample. We selected all of the carbon stars with $3 < J - K < 4$ in the extensive catalogue of CO observations of evolved stars by Loup et al. (1993). Fig. 1 compares the distribution of expansion velocities in the two samples. The Halo carbon stars clearly have a lower mean expansion velocity.

The three stars in the Halo and the Sgr dSph stream have $V_{\rm exp}$ in the range 3–8.5 km s^{-1}, while the three stars associated with the thick disc have velocities ranging from 11.5 to 16.5 km s^{-1}. The latter range is at the low-end of expansion velocities for AGB stars with similar near-infrared colours in the thin disc.

6.5 Origin of the low expansion velocities

Sections 6.3 and 6.4 have shown that the three stars we observed in the Halo and Sgr dSph stream have low expansion velocities. The stars we observed in the thick disc have expansion velocities intermediate between those typically observed in the Halo and the thin disc. This difference could arise from differences in metallicity, with the more metal-poor carbon stars having the slower winds.

Mattsson et al. (2008) and Wachter et al. (2008) have recently conducted theoretical investigations of the winds from metal-poor carbon stars. Both studies show that metal-poor carbon stars can develop high mass loss rates, leading to the formation of a large dusty envelope, in agreement with spectroscopic observations from *Spitzer* of AGB stars in metal-poor galaxies (Sloan et al. 2006; Zijlstra et al. 2006; Groenewegen et al. 2007; Lagadec et al. 2007; Matsuura et al. 2007; Leisenring et al. 2008; Lagadec et al. 2009; Sloan et al. 2009).

Wachter et al. (2008) predict that the outflow velocities from carbon stars should be lower in metal-poor environments because of the lower gas-to-dust mass ratio and because the formation of less dust leads to less efficient acceleration of the wind outside of the sonic region. This interpretation is consistent with our interpretation that the low expansion velocities we have observed in the Halo are due to their low metallicities.

Hydrodynamical models (Winters et al. 2000; Wachter et al. 2008) distinguish two types of models. Model A applies to cases where the radiation pressure on dust is efficient. Mass-loss rates can exceed $10^{-7}\,M_{\odot}\,yr^{-1}$, and expansion velocities can climb above $\sim 5\,km\,s^{-1}$. Model B applies to cases where pulsations drive the mass-loss. In these cases, the mass-loss rates and expansion velocities are smaller. The mass-loss occurs in a two-step process, with stars first losing mass due to pulsations, followed by acceleration due to radiation pressure on the dust grains. The high mass-loss rate and low expansion velocity of TI 32 does not fit either of these models, possibly because metal-poor carbon stars can develop strong mass-loss from pulsation alone.

7 CONCLUSIONS AND PERSPECTIVES

We have detected the CO $J = 3 \rightarrow 2$ in six carbon stars selected as Halo stars. Only one carbon star had been detected in CO previously. Comparison of the infrared observations and radiative transfer models indicates that these stars are losing mass and producing dust. Their mass-loss rates are larger than their nuclear burning rates, so their final evolution will be driven by this mass-loss phenomenon.

We show that three of the observed stars are certainly members of the thick disc, while one is in the Sgr dSph stream and two are in the Halo. The CO observation of the Sgr dSph stream star is thus the first identified millimetre observations of an extragalactic AGB star. The expansion velocity we determined from our CO observations is lower than those of carbon stars in the thin disc with similar near-infrared colours. The observed carbon stars with the lowest expansion velocities are Halo or Sgr dSph stream carbon stars. There is a strong indication that the expansion winds are lower in metal-poor environments, which agrees with recent theoretical models (Wachter et al. 2008).

So far, the effect of metallicity on the mass-loss from carbon-rich AGB stars has studied primarily from infrared observations of AGB stars in Local Group galaxies, mostly with the *Spitzer Space Telescope*. Infrared observations measure the infrared excess, which can be converted to a mass-loss rates assuming an expansion velocity for the circumstellar material. So far all of the mass-loss rates have been estimated using the assumptions that the expansion velocity is independent of the metallicity. The results presented here show that this assumption needs to be reconsidered.

We have recently obtained spectra of some of the present sample with the Infrared Spectrograph on *Spitzer*. Combining our CO observations and these spectra together and comparing them to *Spitzer* spectra from carbon stars in other galaxies in the Local Group will allow us to quantitatively study the mass-loss from carbon-rich AGB stars in the Local Group and its dependence on metallicity. This will be the subject of a forthcoming paper.

ACKNOWLEDGMENTS

EL wishes to thank the JAC staff for their great help carrying out this program, and Rodrigo Ibata for useful discussions about membership of stars to the Sgr stream. we thank the referee C. Loup for her useful comments that helped improving the quality of the paper.

REFERENCES

Beichman C. A., Chester T., Gillett F. C., Low F. J., Matthews K., Neugebauer G., 1990, AJ, 99, 1569
Bowen G. H., Willson L. A., 1991, ApJ, 375, 53
Buchanan C. L., Kastner J. H., Forrest W. J., Hrivnak B. J., Sahai R., Egan M., Frank A., Barnbaum C., 2006, ApJ, 132, 1890
Feast M. W., Whitelock P. A., Menzies J. W., 2006, MNRAS, 369, 791
Groenewegen M. A. T., Oudmaijer R. D., Ludwig H.-G., 1997, A&A, 292, 686
Groenewegen M. A. T. et al., 2007, MNRAS, 376, 313
Hanner M., 1988, Infrared Observations of Comets Halley and Wilson and Properties of the Grains. NASA, Washington
Ibata R., Lewis G. F., Irwin M., Totten E., Quinn T., 2001, ApJ, 551, 294
Ivezic Z., Elitzur M., 1997, MNRAS, 287, 799
Knapp G. R., Morris M., 1985, ApJ, 292, 640
Lagadec E., Zijlstra A. A., 2008, MNRAS, 390, L59
Lagadec E. et al., 2007, MNRAS, 376, 1270
Lagadec E., Zijlstra A. A., Matsuura M., Menzies J. W., van Loon J. T., Whitelock P. A., 2008, MNRAS, 383, 399
Lagadec E. et al., 2009, MNRAS, 396, 598
Leisenring J. M., Kemper F., Sloan G. C., 2008, ApJ, 681, 1557
Loidl R., Lançon A., Jørgensen U. G., 2001, A&A, 371, 1065
Loup C., Forveille T., Omont A., Paul J. F., 1993, A&AS, 99, 291
Marshall J. R., van Loon J. T., Matsuura M., Wood P. R., Zijlstra A. A., Whitelock P. A., 2004, MNRAS, 355, 1348
Mathis J. S., Rumpl W., Nordsieck K. H., 1997, ApJ, 217, 425
Matsuura M. et al., 2007, MNRAS, 382, 1889
Mattsson L., Wahlin R., Höfner S., Eriksson K., 2008, A&A, 484, L5
Mauron N., 2008, A&A, 482, 151
Mauron N., Azzopardi M., Gigoyan K., Kendall T. R., 2004, A&A, 418, 77
Mauron N., Kendall T. R., Gigoyan K., 2005, A&A, 438, 867
Mauron N., Kendall T. R., Gigoyan K., 2007, A&A, 475, 843
Pégourié B., 1988, A&A, 194, 335
Schöier F. L., 2007, in Kerschbaum F., Charbonnel C., Wing R. F., eds, ASP Conf. Ser. Vol. 378, Why Galaxies Care About AGB Stars: Their Importance as Actors and Probes. Astron. Soc. Pac., San Francisco, p. 216
Sloan G. C., Kraemer K. E., Matsuura M., Wood P. R., Price S. D., Egan M. P., 2006, ApJ, 645, 1118
Sloan G. C., Kraemer K. E., Wood P. R., Zijlstra A. A., Bernard-Salas J., Devost D., Houck J. R., 2008, ApJ, 686, 1056
Sloan G. C. et al., 2009, Sci, 323, 353
Smith H. et al., 2008, in Duncan W. D., Holland W. S., Withington S., Zmuidzinas J., eds, Proc. SPIE 7020, Millimeter and Submillimeter Detectors and Instrumentation for Astronomy IV. SPIE, Bellingham, p. 24
Soubiran C., Bienaymé O., Siebert A., 2003, A&A, 398, 141
Totten E. J., Irwin M. J., 1998, MNRAS, 294, 1
Van de Bergh S., 2000, The Galaxies of the Local Group. Cambridge Univ. Press, Cambridge
van Loon J. Th., Zijlstra A. A., Groenewegen M. A. T., 1999, A&A, 346, 805
Wachter A., Winters J. M., Schröder K.-P., Sedlmayr E., 2008, A&A, 486, 497
Whitelock P., Menzies J., Feast M., Marang F., Carter B., Roberts G., Catchpole R., Chapman J., 1994, MNRAS, 267, 711
Whitelock P. A., Feast M. W., Marang F., Groenewegen M. A. T., 2006, MNRAS, 369, 751
Woźniak P. R. et al., 2004, AJ, 127, 2436
Winters J. M., Le Bertre T., Jeong K. S., Helling C., Sedlmayer E., 2000, A&A, 361, 641
Zijlstra A. A., 2004, MNRAS, 348, L23
Zijlstra A. A. et al., 2006, MNRAS, 370, 1961

This paper has been typeset from a TEX/LATEX file prepared by the author.